

Impact of uncertain geology in constrained geophysical inversion

Jeremie Giraud*

*Centre for Exploration
Targeting, School of Earth
Sciences (University of
Western Australia)
35, Stirling Highway
WA Crawley 6009, Australia
Jeremie.giraud@research.uwa.
edu.au*

Evren Pakyuz-Charrier

*Centre for Exploration
Targeting, School of Earth
Sciences (University of
Western Australia)
35, Stirling Highway
WA Crawley 6009, Australia
evren.pakyuz-
charrier@research.uwa.edu.au*

Vitaliy Ogarko

*Centre for Exploration
Targeting, School of Earth
Sciences (University of
Western Australia)
35, Stirling Highway
WA Crawley 6009, Australia
vitaliy.ogarko@uwa.edu.au*

Mark Jessell

*Centre for Exploration
Targeting, School of Earth
Sciences (University of
Western Australia)
35, Stirling Highway
WA Crawley 6009, Australia
mark.jessell@uwa.edu.au*

Mark Lindsay

*Centre for Exploration
Targeting School of Earth
Sciences (University of
Western Australia)
35, Stirling Highway
WA Crawley 6009, Australia
mark.lindsay@uwa.edu.au*

Roland Martin

*Géoscience Environnement
Toulouse
Observatoire Midi-Pyrénées
14 Avenue Edouard Belin
31400 Toulouse, France
roland.martin@get.obs-mip.fr*

SUMMARY

The integration of geological modelling, petrophysics and geophysics in a single inversion scheme is a complex and powerful strategy for solving challenges faced in geoscientific resource exploration. Probabilistic geological modelling and geophysical inversion are non-linear processes that show various degrees of sensitivity to uncertainty in input measurements. Using field geological measurements from the Mansfield area (Victoria, Australia) and synthetic geophysical data, we present a synthetic case study investigating the impact of geological uncertainty on constrained joint geophysical inversion. We investigate the influence of uncertain geological measurements on geologically constrained inversion through a sensitivity analysis to uncertainty in orientation data. Probabilistic geological models used to define constraints for geophysical joint inversion are obtained through a Monte-Carlo based uncertainty estimation (MCUE) method. We simulate a broad range of possible cases through a parameter sweep on uncertainty levels in geological measurements to provide a reference for practitioners. The analysis and comparison of the results at varying uncertainty levels show that results can be grouped into two main categories. For the highest uncertainty levels, significant portions of the models retain the characteristic features of geologically unconstrained inversions. Meanwhile, below a threshold in uncertainty level, inversion benefits from the interaction of geophysical data and geologically conditioned constraints. In such cases, inverted models are improved compared to both the geological modelling alone and geologically unconstrained inversion. The conclusion of this work is that knowledge of this threshold is critical for the interpretation of results and decision making because it indicates whether the datasets provide enough information to take advantage of the complementarities between geological modelling and geophysical inversion. Knowledge of this threshold can also support decision making pertaining to inversion strategies and geological field data collection.

Key words: inversion; geophysical integration; sensitivity analysis; geological modelling.

INTRODUCTION

In the past decade, the integration of different geophysical techniques has been of growing importance in geophysical resource exploration due to the need to exploit complementarities between exploration techniques in increasingly challenging scenarios. Previous studies have focused on joint inversion techniques using constraints enforcing structural similarity between the different models (Gallardo and Meju, 2003; Colombo and De Stefano, 2007), or the use of constitutive petrophysical laws to link the different domains (Gao et al., 2012).

More recently, Sun and Li (2012, 2016) have introduced clustering algorithms as a means of enforcing similarities between the inverted model and prior petrophysical data. Zhang and Revil (2015), and more recently Bijani et al. (2017) and Giraud et al. (2016 and 2017) integrate petrophysics and geology in joint inversion and demonstrate the advantages of integration and joint inversion. However, even if the goal of the aforementioned methods is to obtain better-constrained models, little work has been done to quantify the impact of uncertainty in non-geophysical sources of information used to derive constraints accounting for geological information (Reid et al., 2013).

In this extended abstract, we present a study of the sensitivity of integrated geophysical inversion to uncertainty in geological measurements. Using quality and similarity indicators, we characterize the response of inverted models to varying geological uncertainty. Knowledge of the dependency of constrained inversion to the uncertainty of input geological data is key to guide geoscientists during inversion result interpretation, survey design or project management. In this study we first introduce the inverse modelling approach in three steps (i) the objective function, (ii) we explain how the probabilistic geological model (PGM) is obtained and (iii) how it is used to condition petrophysical constraints. In the second section, we introduce our synthetic case study. The third and last section presents and illustrates the findings of the study.

MODELLING APPROACH

Inversion framework

We formulate the inverse problem in a least-squares sense using the framework introduced by Tarantola and Valette (1982). Let the objective function we minimize be:

$$\theta(\mathbf{m}) = \underbrace{(\mathbf{m}_0 - \mathbf{m})^T \mathbf{C}_m^{-1} (\mathbf{m}_0 - \mathbf{m})}_{\text{model misfit}} + \underbrace{(\mathbf{d} - \mathbf{g}(\mathbf{m}))^T \mathbf{C}_d^{-1} (\mathbf{d} - \mathbf{g}(\mathbf{m}))}_{\text{data misfit}} + \underbrace{\theta_c(\mathbf{P}(\mathbf{m}))}_{\text{constraints}}, \quad (1)$$

where $\theta(\mathbf{m})$ is the function to be minimised. \mathbf{m} represents the inverted model while \mathbf{d} represents the measurements. \mathbf{g} is the operator that calculates the data \mathbf{m} produces. \mathbf{m}_0 is the starting model. \mathbf{C}_m and \mathbf{C}_d are the model covariance and data covariance matrices, respectively. \mathbf{P} is statistical representation of petrophysical measurements in the area and θ_c is a function of \mathbf{P} giving the constraints to be optimized.

The first two terms in equation (1) relate to model and data misfit, respectively. The third term is a measure of the closeness of the petrophysical values of \mathbf{m} and the lithologies observed in the studied area. With spatial geological conditioning, it acts as a local constraint on inversion.

We minimize $\theta(\mathbf{m})$ using the least-square root algorithm (see Paige and Saunders, 1982) as implemented in the inversion platform TOMOFAST3D (Martin et al., 2013). We extended TOMOFAST3D to the joint inversion of gravity and magnetic data using geologically conditioned petrophysical constraints, implementing in 3D the methodology introduced for 2D scenarios by Giraud et al. (2017).

Monte-Carlo Uncertainty Estimation

MCUE is a heuristic uncertainty propagation method for 3D geological modelling that uses topological rules and structural data as inputs, for which we vary the level of uncertainty (Pakyuz-Charrier et al., 2017). MCUE is a stochastic method which samples probability distributions that are thought to best represent input uncertainty (e.g. a representation of measurement error about geological structural data). This approach produces a suite of geologically plausible models. The error distribution of input orientation data is represented by a von Mises-Fisher distribution (vMF). The parameter of the vMF which we vary here, κ , can be interpreted as the analogous to the inverse of the standard deviation for Gaussian distributions. In our case, using Mardia and Jupp (2000), the vMF can be written as:

$$vMF(x|\gamma, \kappa) = \frac{\kappa}{4\pi \sinh(\kappa)} e^{\kappa \gamma^T x}, \kappa \in \mathbb{R}^+ \text{ and } \|\gamma\| = 1, \quad (2)$$

where x is the vector representing orientation data. T denotes the transpose operator. γ is the mean direction vector. κ , the parameter we study here, is called the concentration parameter. It is analogous to the inverse of the standard deviation for normal distributions.

The suite of plausible models is combined into a PGM that records the probabilities of each geological model over a 3D grid. For the i -th cell of the medium, the probability of rock unit j is given by $\psi_{j,i}$, with $\sum_{j=1}^{n_l} \psi_{j,i} = 1$. If the geological dataset is perfectly constrained, the PGM reduces to the original geological model. For sufficiently uncertain data, all units are nearly equiprobable. Examples displayed in Figure 1 show the probability cube obtained for the basement lithology, with $\kappa = 4$, 20 and $\kappa = 90$, equivalent to decreasing levels of uncertainty in the measurements.

Geologically conditioned petrophysical constraints

To maximize the similarity between the statistical properties of the measured petrophysical data and the inverted model we follow concepts introduced by Sun and Li (2012, 2016) and Lelièvre et al. (2012) and condition the petrophysical constraints geologically following Giraud et al. (2017):

$$\mathbf{P}(\mathbf{m}) = \begin{bmatrix} P_1(m_1) \\ P_2(m_2) \\ \dots \\ P_{n_m}(m_{n_m}) \end{bmatrix}, \text{ with } P_i(m_i) = \sum_{k=1}^{n_l} \psi_{k,i} N(m_i | \boldsymbol{\mu}_k, \boldsymbol{\sigma}_k), \quad (3)$$

In equation (3), each normal distribution N is characterized by a mean value vector, $\boldsymbol{\mu}_k$, which corresponds to the mean value for the k -th lithology, and the associated covariance matrix, $\boldsymbol{\sigma}_k$. $\psi_{k,i}$ is the relative weight of the k -th lithology in the i -th cell that is extracted from the probabilistic geological model. The parameters $\boldsymbol{\sigma}_k$ and $\boldsymbol{\mu}_k$, are estimated from petrophysical measurements in the area. Once $\psi_{k,i}$ and N are computed, the starting model \mathbf{m}_0 is derived from the mathematical expectation of \mathbf{P} .

SENSITIVITY ANALYSIS

Test model

We built the 3D unperturbed geological model from surface orientation (foliations) and contact (interface points) data collected in the Mansfield area (Victoria, Australia). It presents a Carboniferous sedimentary syncline oriented N170, abutting a faulted contact with a folded ultramafic basement. The complexity of the model was artificially increased to better test the inversion algorithm through the addition of a fictitious north-south fault and of a mafic intrusion to the south-west. The original Mansfield model can be found as part of the GeoModeller installation (Tutorial case study H). Figure 2 shows the resulting magnetic susceptibility and density contrast. Figure 3 shows the statistical petrophysics when all lithologies are unweighted and equiprobable (e.g., all $\psi_{k,i}$ equal to 1/6 as there are 6 lithologies in our model).

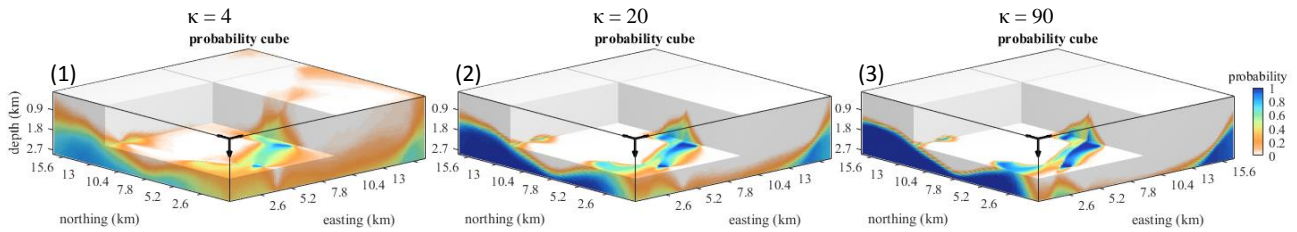


Figure 1 – Comparison of probabilities of a given voxel belonging to the basement lithology class for different κ values.

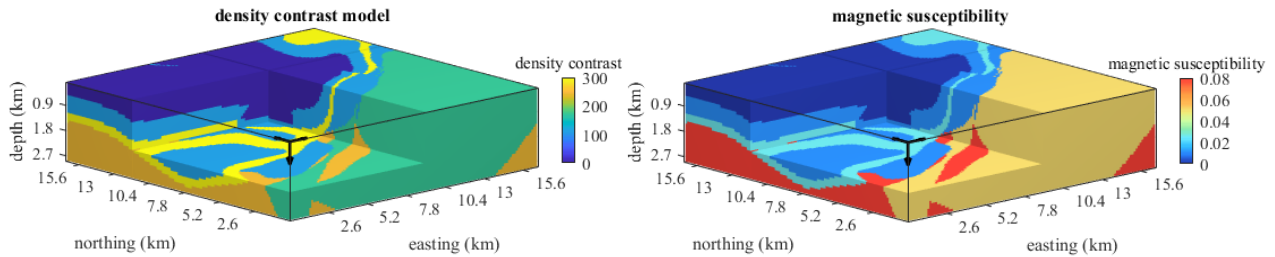


Figure 2 – Unperturbed (or true) model, density contrast (in kg per cubic meter) and magnetic susceptibility (SI).

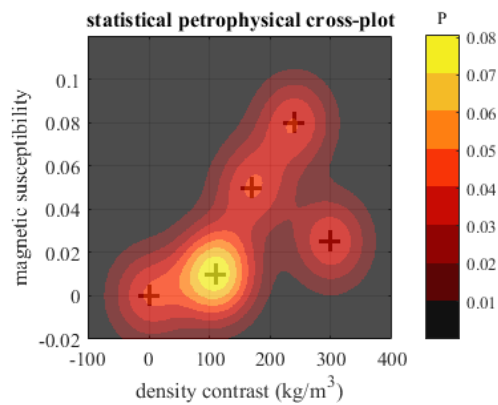


Figure 3 – Petrophysical model. Crosses symbolize the centre of Gaussians defining N used to derive the petrophysical constraints. The brighter values corresponds to the case where two lithologies have the same properties.

Orientation parameter

We generated a series of probabilistic geological models using uncertainty levels on orientations with κ ranging between 0.1 and 200. We made the hypothesis that uncertainty on for the interfaces' locations was equal to 50m (isotropic and uniform) for all simulations. Figure 1 shows the probability model obtained for the cases $\kappa = 4, 20$, and 90 , corresponding to cases level where 99% of the data lies within 52, 22 and 12.5 degrees aperture cones, respectively. The tested uncertainty levels range from values corresponding to high quality field data ($\kappa = 200$, e.g., 7 degrees aperture cone) to highly uncertain, poor quality field data ($\kappa < 10$), to nearly void of information measurements ($\kappa = 0.1$, 160 degrees aperture cone) with maximum uncertainty.

Quality and similarity indicators

We characterize the distance between inverted and true models using the root-mean-square (RMS) misfit between true and inverted models. We also compare spatial variations of inverted and true models by calculating the cosine between their respective spatial gradients. To complement the analysis, we calculate the different components of the Structural SIMilarity index (SSIM, Wang et al., 2004). The SSIM index is the products of three terms, which characterise the closeness between inverted and true models in terms of "texture", "contrast", and "structure".

RESULTS

Comparisons of inverted models demonstrates that below a threshold of $\kappa=20$, the geology of inverted models (Figure 4) is inconsistent with that of the true model even if inversion results are better than for unconstrained inversion. This knowledge is critical for sound interpretation and decision making. This is illustrated in Figure 4, where the different portions of the high-density contrast lithology reconnect for $\kappa = 20$ (arrow) for both density contrast and magnetic susceptibility models. In addition, for κ lower than 4, results obtained from constrained inversion become very similar to unconstrained inversions. As pointed out in Giraud et al. (2017) and references therein, geophysical data misfit in joint inversion exhibits little sensitivity to the level of integration due to the non-uniqueness of the inversion problem. For this reason, we do not show the evolution geophysical data misfit in this document. The SSIM indicator and the RMS model misfit (Figure 5) display rapid improvement of inversion result quality with increasing κ . For example, with $\kappa=1$, SSIM and RMS indicate significantly improved inversion results compared to unconstrained inversions.

Nevertheless, improvements in terms of similarity between inverted and true models decrease rapidly for $\kappa \geq 20$ to near stationarity for $\kappa \geq 50$. This suggests that $\kappa = 20$ could be used as a threshold for optimum trade-off between final result quality and data certainty level. It also means that it is necessary to reduce other sources of uncertainty to help increase the closeness between true and inverted models. For example, better constrained petrophysical distributions would increase inverted to true model fidelity.

For lower values of κ , $\kappa = 1$ can be used as a threshold below which the interest of integrating geological information in inverse modelling is limited. This means that for $\kappa < 1$, geological information is too uncertain to be exploited in geophysical inversion.

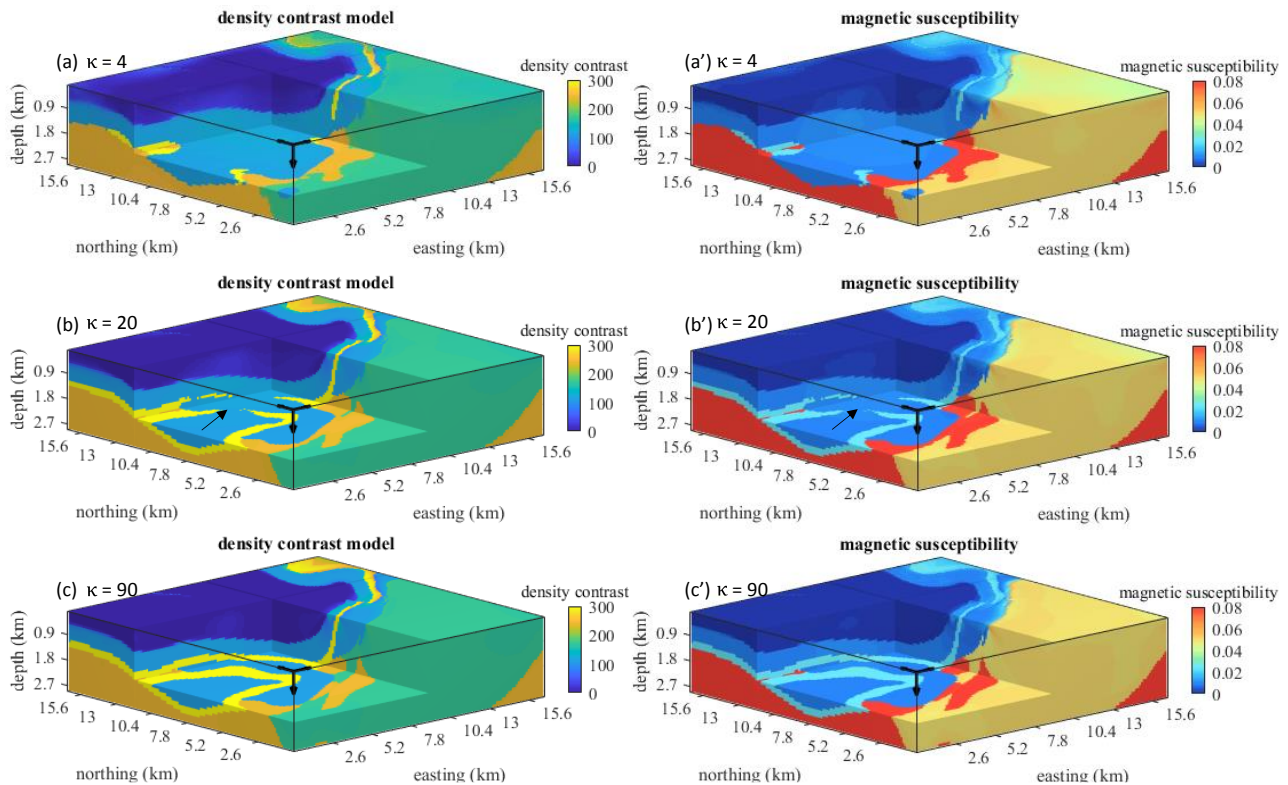


Figure 4 – Comparison of inversion results for kappa 4 (a, top), 20 (b, middle) and 90 (c, bottom).

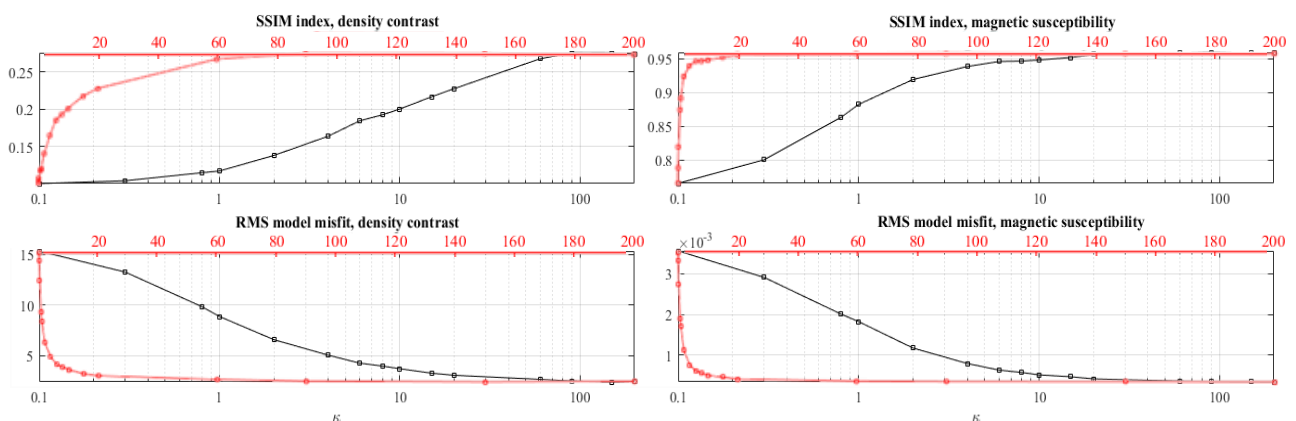


Figure 5 – Plot the Structural SIMilarity (SSIM) index and RMS model misfit for different κ values, represented in log (black) and linear (red) abscissa scale representing κ .

CONCLUSION AND DISCUSSION

The sensitivity analysis of joint inversion to uncertainty in information used to derive constraints illustrates the non-linear relationship between input and prior information uncertainty and inversion quality. It also shows that the use of data containing uncertainty may improve results significantly even for high input uncertainty levels (for example, κ values as low as 1 permit to reduce the RMS model misfit by a factor of 2 with respect to $\kappa = 0.5$). However, it also suggests that, provided the input uncertainty level is lower than a specific threshold ($\kappa \geq 20$), a decrease may not lead to proportional improvement in inversion results. The threshold value $\kappa = 20$ is important for both decision making and interpretation in that (i) results are nearly optimum for $\kappa > 20$, and that (ii) for $20 > \kappa > 1$, efforts in reducing geological input data uncertainty can improve final modelling results quality and uncertainty.

Current work include the illustration and validation of the work presented here using geological, petrophysical and geophysical data collected in the Yerrida Basin (Western Australia). Current work also extends to the study of the influence of petrophysical measurements quality. Future work include the study of the presented work to other sources of uncertainty, with the aim to create a more comprehensive study of the influence of uncertainty in prior information and constraints on geophysical inversion results.

ACKNOWLEDGMENTS

The authors gratefully acknowledge the high performance computing center CALMIP – Mésocentre de calcul de l'Université Fédérale Toulouse Midi-Pyrénées (Toulouse, France) where the parallel code TOMOFAST3D was run for the purpose of the presented work. The authors thank the Australian Society of Exploration Geophysicists Research Foundation for their support to the PhD project related to the presented work. The authors are thankful to the Geological Survey of Western Australia, the Australian Research Council, the Australian Federal government and the Western Australian Fellowship Program for their financial support. They also thank Darren Hunt from Teck Resources for fruitful discussions.

REFERENCES

- Bijani, B., Lelievre, P. G., Ponte-Neto, C. F., and Farquharson, C. G., 2017, Physical-property-, lithology- and surface-geometry-based joint inversion using Pareto Multi-Objective Global Optimization, *Geophysical Journal International*, 209, 730–748.
- Colombo, D., and de Stefano, M., 2007, Geophysical modeling via Simultaneous Joint Inversion of seismic, gravity and electromagnetic data: Application to pre-stack depth imaging: *The Leading Edge*, 26, no. 3, pp. 326-331. DOI: 10.1190/1.2715057.
- Gallardo, L., and Meju, M. A., 2003, Characterization of heterogeneous near-surface materials by joint 2D inversion of dc resistivity and seismic data: *Geophysical Research Letters*, 30, no 13, 1-1 – 1-4, doi:10.1029/2003GL017370.
- Gao, G., Abubakar, A., Habashy, T. M., and Pan, G., 2012b, joint petrophysical inversion of electromagnetic and full-waveform seismic data: *Geophysics*, 77, no. 3, PWA3-WA18, doi: 10.1190/GEO2011-0157.1.
- Giraud, J., Pakyuz-Charrier, E., Jessell, M., Lindsay, M., Martin, R., and Ogarko, V., 2017, Uncertainty reduction through geologically conditioned petrophysical constraints in joint inversion. *GEOPHYSICS* (accepted). <https://doi.org/10.1190/geo2016-0615.1>.
- Giraud, J., Jessell, M., Lindsay, M., Martin, R., and Pakyuz-Charrier, E., 2016, Integrated geophysical joint inversion using petrophysical constraints and geological modelling, Extended Abstract, SEG Annual Meeting Dallas 2016, doi: 10.1190/segam2016-13945549.1
- Lelièvre, P. G., Farquharson, C., and Hurich, C. A., 2012, Joint inversion of seismic traveltimes and gravity data on unstructured grids with application to mineral exploration: *Geophysics*, 77, no. 1, P.K1-K15, doi: 10.1190/GEO2011-0154.1.
- Mardia, K. V., and Jupp, P., 2000, *Directional Statistics* (2nd ed.). John Wiley and Sons Ltd.
- Martin, R., Monteiller, V., Komatitsch, D., Perrouy, S., Jessell, M., Bonvalot, S., and Lindsay, M., 2013, Gravity inversion using wavelet-based compression on parallel hybrid CPU/GPU systems: application to southwest Ghana: *Geophysical Journal International*, 195, no. 3, 1594-1619, doi: 10.1093/gji/ggt334.
- Paige, C. C., and Saunders, M. A., 1982, LSQR: An algorithm for sparse linear equations and sparse least squares, *TOMS* 8(1), 43-71.
- Pakyuz-Charrier, E., Giraud, J., Lindsay, M., and Jessell, M., 2017, Common Uncertainty Research Explorer uncertainty estimation in geological 3D modeling, Expanded abstract, Mineral Prospectivity, current approaches and future innovations – Orléans, France, 24-26 October 2017.
- Reid, A., O'Callaghan, S. T., Bonilla, E. V., McCalman, L., Rawling, T., and Ramos, F., 2013, Bayesian Joint Inversions for the Exploration of Earth Resources: Proceedings of the twenty-third international joint conference on artificial intelligence, P.2877-2884, doi: 10.1.1.415.9471.
- Sun, J., and Li, Y., 2013, A general framework for joint inversion with petrophysical information as constraints: SEG 83rd Annual Meeting, SEG, Expanded Abstract, pp. 3093-3097, doi: 10.1190/segam2013-1185.1.
- Sun, J., and Li, Y., 2016, Joint inversion of multiple geophysical and petrophysical data using generalized fuzzy clustering algorithms: *Geophysical Journal International*, 208, 1201–1216, doi: 10.1093/gji/ggw442.
- Wang, Z., Bovik, A.C., Sheikh, H.R., Simoncelli, E.P., 2004, Image quality assessment: from error visibility to structural similarity, *IEEE Transactions on Image Processing*. 13 (4), 600–612, doi:10.1109/TIP.2003.819861.
- Zhang, J., and Revil, A., 2015, 2D joint inversion of geophysical data using petrophysical clustering and facies deformation: *Geophysics*, 80, no. 5, M69-M88, doi: 10.1190/GEO2015-0147.1.